CrossMark

RESEARCH ARTICLE

Heavy metals in the gold mine soil of the upstream area of a metropolitan drinking water source

Huaijian Ding[1] · Hongbing Ji[1,2] · Lei Tang[1,3] · Aixing Zhang[1] · Xinyue Guo[1] · Cai Li[1] ·
Yang Gao[1] · Mergem Briki[1]

Abstract Pinggu District is adjacent to the county of Miyun, which contains the largest drinking water source of Beijing (Miyun Reservoir). The Wanzhuang gold field and tailing deposits are located in Pinggu, threatening Beijing's drinking water security. In this study, soil samples were collected from the surface of the mining area and the tailings piles and analyzed for physical and chemical properties, as well as heavy metal contents and particle size fraction to study the relationship between degree of pollution degree and particle size. Most metal concentrations in the gold mine soil samples exceeded the background levels in Beijing. The spatial distribution of As, Cd, Cu, Pb, and Zn was the same, while that of Cr and Ni was relatively similar. Trace element concentrations increased in larger particles, decreased in the 50–74 μm size fraction, and were lowest in the <2 μm size fraction. Multivariate analysis showed that Cu, Cd, Zn, and Pb originated from anthropogenic sources, while Cr, Ni, and Sc were of natural origin. The geo-accumulation index indicated serious Pb, As, and Cd pollution, but moderate to no Ni, Cr, and Hg pollution. The Tucker 3 model revealed three factors for particle fractions, metals, and samples. There were two factors in model A and three factors for both the metals and samples (models B and C, respectively). The potential ecological risk index shows that most of the study areas have very high potential ecological risk, a small portion has high potential ecological risk, and only a few sampling points on the perimeter have moderate ecological risk, with higher risk closer to the mining area.

Keywords Mine soil · Heavy metals · Source identification · Risk assessment · Multivariate analysis · Tucker 3 model

Introduction

Contamination of soil environments with metals from anthropogenic sources is an important global issue (Sterckeman et al. 2000; Acosta et al. 2011). During mining, metals in tailings and the surrounding rock are left in the surroundings and accumulate in the soil, causing heavy metal pollution, which is latent, cumulative, long term, and recalcitrant. Additionally, it is possible for heavy metals accumulated in soil to migrate into vegetation and, subsequently, the human body via the food chain or groundwater, thereby affecting human health (Li et al. 2014; Zhuang et al. 2009). Currently, most studies are focused on the polluting characteristics of heavy metals in metal mines (Guo et al. 2011; Liu et al. 2010), while there were few investigations of heavy metals in environmentally sensitive areas, such as those containing important drinking water sources. Therefore, this study was conducted to investigate soil pollution of an important

1 Civil and Environmental Engineering School, University of Science and Technology Beijing, Xueyuan Road No.30, Haidian District, Beijing 100083, People's Republic of China

2 State Key Laboratory of Environmental Geochemistry, Institute of Geochemistry, Chinese Academy of Sciences, Guiyang 550002, People's Republic of China

3 Beijing Geological Engineering Design and Research Institute, Beijing 101500, People's Republic of China

drinking water source region by heavy metals originating from the tailings of closed mines.

Soil particle size is an important factor influencing the mobility of trace elements. Since the 1980s, many studies have investigated the distribution of particle size of trace elements in surface soil (Ahmed and Ishiga 2006; Viklander 1998). Because of the erosion, ease of transport and size of specific surface area, etc., the concentration (Förstner and Wittmann 2012), migration, and transformation of trace element pollutants are all closely related to particle size, with fine particulate matter acting as a carrier for trace elements in soils, bringing potential risks to the environment and human health (Dominici et al. 2006; Vallejo et al. 2006). The concentrations of trace elements in soils increase with decreasing particle size because fine particles have a greater specific surface area, and most of them were negative charge, high clay content, and high organic content (Baek et al. 1997; Barberis et al. 1991; Charlesworth and Lees 1999). Different types of clay minerals, particularly montmorillonite, kaolinite, and illite, also adsorb trace elements (Brady and Weil 1996). Research and evaluation of the activity and potential environmental risk generated by trace elements in different size fraction components can further strengthen our understanding of the transfer and transformation of trace elements and may provide strategies to repair and control the pollution.

The primary objective of the study was to examine heavy metals in a gold ore area near the Zhongqiao water source in Pinggu. To accomplish this, we collected soil samples typical of gold ore mining and established the source and distribution of trace elements in the region through clustering analysis and principal component analysis (PCA), Furthermore, we investigated the level of trace element pollution by applying a geo-accumulation index (I_{geo}), while the relationship between the contents of heavy metals, particle size distribution of soil, and the distribution of the space was studied by the Tucker 3 model. The results presented herein provide a scientific basis for preventing and controlling heavy metals contamination.

Materials and methods

Study area

Beijing has recently undergone very rapid development that has included transformation into a political and cultural center. The metropolis with more than 20,000,000 population only has one major source of drinking water, the Miyun Reservoir. Drinking water safety is the top priority of urban development. The Zhongqiao water source in the Pinggu District of Beijing serves as an emergency water source; accordingly, its quality directly affects the safety of water in Beijing. The Pinggu district is located about 70 km northeast of downtown Beijing. The District covers an area of 1075 km^2, 59.7 % of which is mountain area. Pinggu has a warm temperate continental monsoon climate, with hot and rainy summers and cool and humid autumns. The average maximum temperature is 17.3 °C, while the average annual rainfall is about 644 mm.

Upstream of the Zhongqiao water source is abundant gold resources. Although smelting activities in Wanzhuang gold mining area are now closed, they have influenced the soil surrounding the water sources. In this study, we collected and analyzed soil from Wanzhuang tailings and the surrounding areas.

Sampling and analytical methods

Gold mining process in the study area generated a lot of waste rock, deposited on the slopes, and trench freely, without any interception measures. Consider the mining lot, tailing pond, transportation route of peripheral ore mining area, and the position of the residential areas. Combining with the local terrain, we avoid the crowds to sample as far as possible. A total of 25 soil samples were collected from 25 locations (P1–P25) in the Wanzhuang mining area according to the sampling grid shown in Fig. 1. GPS was used to locate the sample points throughout the survey process. Samples were placed in labeled polyethylene bags for transport to the laboratory, where they were air-dried, gently crushed, and sieved at 2 mm with a plastic sieve and then ground, homogenized with an agate mortar, and sieved again through a mesh sieve (<2 mm) for laboratory analyses.

We selected the first 10 samples (p1∼p10) around KongChengYu village, then the samples were partitioned into five size fractions : <2, 2–5, 5–10, 10–50, and 50–74 μm. For separation, air-dried soil samples were passed through a 200 mesh sieve (74 μm). Next, 100 g of soil from the 200 mesh sieve was dispersed with Na-hexametaphosphate for 16 h by horizontal shaking. The <2 μm fraction was separated by centrifugation, after which the remaining fractions were subjected to repeated sedimentation and decanting. Following separation, all the fractions were dried and weighted.

Total concentration of heavy metals

Soil samples were analyzed for their chemical and physical properties. The pH was determined potentiometrically in a soil–CaCl$_2$ (0.01 M) suspension (soil/solution 1:5, ISO
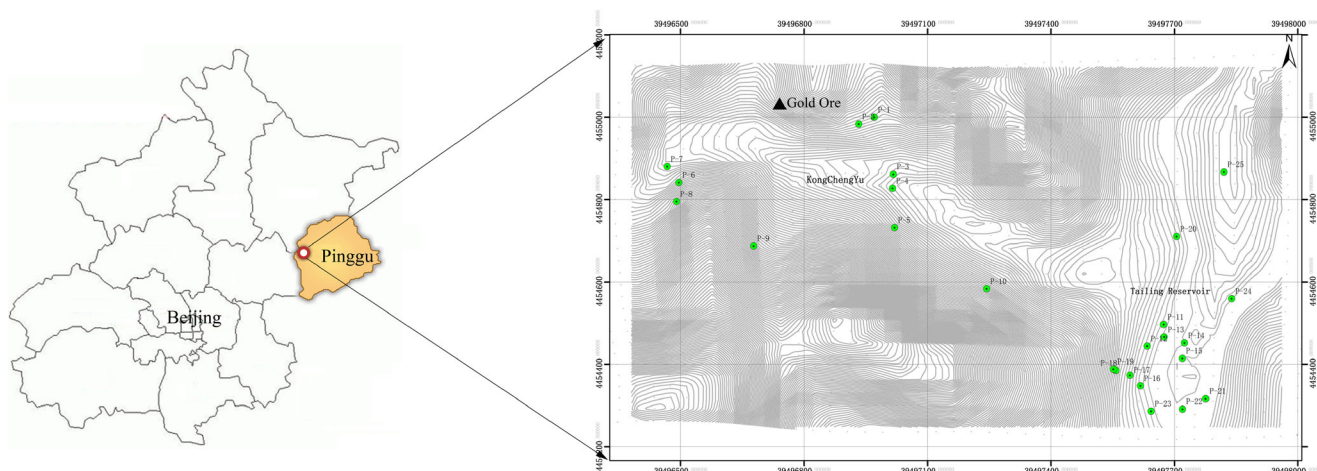
Fig. 1 Schematic map of the study area and sampling points

10390). The total organic carbon content was measured using a TOC analyzer (Elementar Company, Germany).

The concentrations of Cu, Zn, Cd, Cr, Ni, and Pb were determined for bulk soil samples and size fractions by inductively coupled plasma mass spectrometry. Briefly, samples (0.10 g) were placed into a Teflon beaker, after which 1.5 ml HF, 1 ml HNO_3, and 2 ml H_2O_2 were added. The beaker was then placed on a hot plate (~140 °C) for 48 h until the sample was completely dissolved and vaporized to dryness. Next, 1 ml HNO_3 was added with an appropriate amount of ultrapure water, and the mixture was heated so that the salts dissolved completely. The resulting solution was placed in a 50-ml plastic bottle and measured against the internal standard. All analyses were conducted alongside standards.

In addition, 0.3000 g of sieved sample was added to 10 mL fresh HCl/HNO_3 (v/v=3:1) and placed in a 95 °C water bath for 2 h, during which time it was hand shaken four times (Li 2004). Once it had cooled, the digestion solution was then diluted to 50 mL by ultrapure water (resistivity = 18.2 MΩcm^{-1}). Next, 25 mL of dilute solution was removed, mixed with 5 mL HCl (1.19 g mL^{-1}), and 5 mL solution of CH_4N_2S (50 g L^{-1}) and diluted to 50 mL. Finally, the sample was allowed to stand for 30 min, after which the dilute solution was analyzed by Atomic Fluorescence Spectrometry (AFS-920, Ji Tian) for As and Hg.

Multivariate statistical method

Multivariate statistical methods offer powerful tools for monitoring soil properties. Such methods have been widely applied to investigate the concentration, accumulation, and distribution of trace elements in soils (Lin et al. 2002; Qishlaqi and Moore 2007; Salman and Ruka'h 1999), as well as the behavior, distribution, and interrelationship of trace elements in soils.

Principal component analysis (PCA) can reduce the complexity of large-scale data sets and are broadly used in environmental impact studies (Perona et al. 1999) to elucidate the relationships among variables by identifying common underlying processes (Farnham et al. 2003; Webster and Oliver 1990). The number of significant principal components was selected on the basis of a Kaiser criterion of eigenvalues higher than 1 (Kaiser 1960) and a total explained variance equal to or higher than 85 %.

Cluster analysis (CA) is often coupled with PCA to check results and group individual parameters and variables (Facchinelli et al. 2001). Cluster analysis (CA) is a group of multivariate techniques that allows the assembly of objects based on their characteristics. CA classifies objects so that each is similar to others in the cluster with respect to a predetermined selection criterion. Hierarchical agglomerative clustering, which is the most common approach, provides intuitive similarity relationships between any one variable and the entire data set and is typically illustrated by a dendrogram.

Because data describing particle size fractions are always compiled in tridimensional or higher arrays, it is not possible to analyze the environmental characteristics of particle fractions directly. Accordingly, PCA and other two-way approaches cannot identify complicated relationships in the surroundings well. Therefore, Stanimirova et al. (2006) developed a more advanced technique known as the Tucker N-way to analyze data sets arranged in groups of three or more. Furthermore, Stanimirova postulated that more advanced methods such as the Tucker N-way will become more popular in the future. Pardo et al. (2008) used two-way and N-way PCA to analyze heavy metal data and found that the Tucker 3 model provided more detailed information for use in the development of remediation strategies for contaminated soil and sediment. Ding and Ji (2010) and Huang et al. (2013) used the

Tucker 3 model to analyze heavy metal fraction data and found more detailed information for contaminated sediment and soil.

Geo-accumulation index

The geo-accumulation index (I_{geo}) introduced by Müller (1969) was used to quantify heavy metal pollution in aquatic sediment. The formula of I_{geo} is as follows:

$$I_{geo} = \log_2(C_n/1.5B_n)$$

where C_n is the measured concentration of metal n, B_n is the background value (average shale) of metal n, and factor 1.5 is the background matrix correlation factor due to lithogenic variation. Seven classes of the geo-accumulation index were suggested by Mülller (1969): class 0 (unpolluted), $I_{geo}<0$; class 1 (unpolluted to moderately polluted), $0<I_{geo}<1$; class 2 (moderately polluted), $1<I_{geo}<2$; class 3 (moderately to heavily polluted), $2\leq I_{geo}<3$; class 4 (heavily polluted), $3\leq I_{geo}<4$; class 5 (heavily to extremely polluted), $4\leq I_{geo}<5$; and class 6 (extremely polluted), $I_{geo}\geq5$.

Potential ecological hazard index

Hakanson (1980) reflects not only the effects of a single trace element in a particular environment, but also the effects of multiple trace elements. He uses quantitative methods to determine the degree of potential ecological hazard and is widely used in pollution assessments of trace elements in soils and sediments. The calculation includes four steps:

1. The contamination factor of a single trace element, or C_r^i is determined by:

$$C_r^i = C_{surface}^i / C_n^i$$

Where $C_{surface}^i$ is the measured concentration of trace elements in the soil (or sediment), and C_n^i is the reference value. The reference value is set as the highest background value of trace elements in sediments in modern preindustrial times as suggested by Hakanson, although some scholars use national soil environmental standard values as the reference.

2. The toxic response factor of trace elements, T_r^i, is used to reflect the response of trace elements in water, sedimentary, and biological phases. A standardized trace element toxic response coefficient was taken as the assessment standard as suggested by Hakanson. The toxic response coefficients were Zn=1<Cr=2<Cu=Ni=Pb=5<As=10<Cd=30<Hg=40 (Xu et al. 2008; Xv et al. 2008);

3. The potential ecological risk index, E_r^i, can then be calculated for each trace element:

$$E_r^i = T_r^i \times C_r^i$$

4. The potential ecological risk index of various trace elements, or RI, can be divided into five levels such that the potential ecological harm is:

$$RI = \sum_{i=1}^{n} E_r^i$$

Results

Soil physical and chemical properties

The pH and organic matter (OM) content of surface soils (0–20 cm) in the area of the Wanzhuang gold ore near Zhongqiao water sources are shown in Table 1. The soil pH is mainly acidic, ranging from pH 3.77 to 6.60. The most acidic was topsoil near the highest altitude and close to the tailings reservoir where the tailings stocked in half hillside directly or filled in natural ditch. This value might reflect the dust and tailings generated by smelting and the acidic mine drainage produced by the gold ore oxidation. The OM contents in the study are arranged from 0.34 to 7.28 %, with the highest found in surface soil from grassland near the gold ore. This may reflect that grassland soils are naturally richer in OM than others. These conclusions are consistent with the results of previous studies (Gao et al. 2012; Huang et al. 2013; Qin et al. 2014).

Total metals content of surface soils

The total heavy metals concentrations in surface soils (0–20 cm) in the Wanzhuang gold mining area are presented in Table 1.

As shown in Table 1, the ratio of the mean/background values in Beijing was in the order Cd>As>Pb>Zn>Cu>Ni>Cr>Hg, with values 53.49, 29.88, 22.42, 3.57, 2.62, 1.37, 1.35, and 0.81 times those of the background value, respectively. The Cd content of P-1, P-2, P-3, P-20, and P-4 was highest. Because there is no nearby farmland and planting areas, there is almost no use of fertilizers; this was likely because P-1–P-4 were closer to the mining area and P-20 was near the tailing reservoir relative to the other sample sites.

Characteristics of soil elements in particle size fractions

The concentrations of Cu, Zn, Cd, Cr, Ni, Pb, Hg, and Y in various size fractions are shown in Table 2 and Fig. 2. Trace

Table 1 Contents of heavy metals and organic carbon, and pH value in bulk samples of surface soils of the study area

Samples	Contents of heavy metals/mg·kg^{-1}								pH	OM
	Cu	Zn	Cd	Cr	Ni	Pb	As	Hg		%
P-1	79.7	1680	14.0	93.5	44.1	6380	2386	0.097	6.55	0.73
P-2	121	2460	23.2	78.8	45.2	2345	1279	0.117	6.68	7.28
P-3	175	1270	14.2	85.2	42.3	932	881	0.038	6.58	2.32
P-4	71.8	472	4.6	104	46.2	335	366	0.024	6.98	0.37
P-5	30	118	0.8	90.2	35.9	91.6	47	0.022	6.89	0.39
P-6	60.8	137	0.6	106	50.3	67.6	36	0.038	6.8	1.7
P-7	163	172	1.1	83.1	35.8	97.4	50	0.038	6.36	0.37
P-8	46.4	118	0.5	93.3	38.6	78	34	0.047	6.4	1.76
P-9	36	118	0.5	86.2	32.7	87.8	57	0.075	7.1	1.87
P-10	60.7	182	1.5	83.2	31	655	316	0.132	6.74	1.05
P-11	49.1	110	0.7	73.7	24.3	361	164	0.057	6.96	0.37
P-12	26.5	72	0.2	95.6	36.3	43.1	40	0.011	6.78	0.46
P-13	46.4	169	1.2	77.9	28.6	426	192	0.038	7.9	1.17
P-14	37.1	88.9	0.6	67.1	23.8	258	130	0.08	7.39	0.6
P-15	27.6	73.8	0.2	86.9	35.1	34.3	22	0.012	7.41	0.34
P-16	35.2	112	0.5	95.6	39.3	136	88	0.02	6.76	0.41
P-17	58.9	118	0.4	177	91.3	96.2	53	0.043	6.66	1.26
P-18	38.8	108	0.5	97.7	45.1	95.6	56	0.04	3.77	1.69
P-19	32.3	90	0.4	92.4	43.8	62.6	39	0.031	6.88	0.89
P-20	106	365	2.8	77.1	31.5	321	213	0.029	6.62	0.49
P-21	39.8	103	0.4	91.4	38.7	78.3	29	0.024	6.69	1.15
P-22	31	98.3	0.4	89.8	33.4	101	49	0.039	6.48	1.33
P-23	46.8	128	0.5	75.7	34.2	95.3	53	0.024	6.55	1.47
P-24	56.4	191	1.0	85.7	34.4	423	271	0.054	6.79	1.24
P-25	35.2	130	1.1	68.8	23	241	171	0.032	6.6	0.88
Minimum	26.5	72	0.2	67.1	23	34.3	22	0.011	3.77	0.34
Maximum	175	2460	23.2	177	91.3	6380	2386	0.132	7.9	7.28
Median	46.4	118	0.6	86.9	35.9	101	57	0.038	6.74	1.05
Mean	60	347	3	90	39	554	281	0.05	6.7	1.3
Background in Beijing[a]	23.1	97.2	0.0534	66.7	28.2	24.7	9.4	0.0576	–	–
Mean/background in Beijing	2.62	3.57	53.49	1.35	1.37	22.42	29.88	0.81	–	–
SD	40.18	582.56	5.67	20.63	13.13	1303.42	525.55	0.03	0.70	1.38
Skewness	1.86	2.83	2.75	3.22	2.74	4.13	3.23	1.49	−2.97	3.72
Kurtosis	2.90	7.67	7.17	13.57	10.84	18.16	11.18	1.75	13.51	16.27

[a] China National Environmental Monitoring Centre. Soil Element Background Values of China[J](in Chinese). China Environmental Science Press, 1990

element concentrations increased in larger particles, decreased in the 50–74 μm size fraction, and were lowest in the <2 μm size fraction.

Application of chemometric analysis

The data obtained from analytical methods were analyzed using SPSS version 16.0 for Windows. Pearson's correlation coefficient analysis, PCA, and cluster analysis (CA) were performed to identify the relationships among soil heavy metals and their possible sources.

PCA and derivative methods have been widely applied to various environmental media, such as soils (Tahri et al. 2005; Zheng et al. 2008; Facchinelli et al. 2001), dust (Meza-Figueroa et al. 2007), and water (Tahri et al. 2005), to identify pollution sources and apportion natural versus anthropogenic contributions. In this study, CA was applied to identify different geochemical groups based on similar heavy metals contents according to the Ward-algorithmic method. The results

Table 2 Contents of heavy metals in particle size fractions samples of surface soils of the study area

Sample	Particle size fractions	Contents of heavy metals/ mg kg^{-1}							
		Cu	Zn	Cd	Cr	Ni	Pb	Y	Hg
P-1	<2 μm	40.6	373	2.8	136	52.1	2324	19.3	0.024
	2–5 μm	62.8	596	4.16	123	70.4	3592	25.6	0.082
	5–10 μm	79.5	767	6.05	157	87.8	4769	30.2	0.080
	10–50 μm	70.2	817	4.95	171	83.2	4317	27.5	0.095
	50–74 μm	76.5	806	5.99	164	88.1	4644	30	0.090
P-2	<2 μm	99.8	1455	17.9	73.3	38.2	1431	19.9	0.187
	2–5 μm	138	2281	21.6	69	42.4	2287	20.9	0.283
	5–10 μm	229	4145	32.3	103	70.3	4200	28.8	0.717
	10–50 μm	244	4887	31.7	118	78.4	3969	31.8	0.771
	50–74 μm	259	5064	33.8	121	81.8	4259	29.2	0.431
P-3	<2 μm	24.6	78.7	0.269	70.4	28.6	52.8	27.7	0.028
	2–5 μm	37.2	121	0.426	90.1	43.7	77.4	33.7	0.061
	5–10 μm	40.5	137	0.491	95.7	48.3	92.6	33.9	0.046
	10–50 μm	45.8	240	0.467	108	55.8	106	36.7	0.043
	50–74 μm	27.5	116	0.239	66.6	31.7	59.7	30	0.033
P-4	<2 μm	42.3	88.2	0.358	61.5	23.9	52.4	25.9	0.052
	2–5 μm	51.4	138	0.426	88	41.2	66.8	33.8	0.096
	5–10 μm	59.9	191	1.01	99.3	54.1	91.6	33.9	0.129
	10–50 μm	67.1	250	0.72	117	63.2	104	40.5	0.148
	50–74 μm	43.8	117	0.565	64.7	26.3	68.2	26.7	0.075
P-5	<2 μm	106	242	2.17	66.4	25.8	1125	23.2	0.115
	2–5 μm	79.8	272	2.39	81	38.9	986	30.2	0.379
	5–10 μm	147	848	2.33	107	53.6	1502	37.6	0.402
	10–50 μm	107	1689	3.05	102	58	1556	41.2	0.419
	50–74 μm	113	617	2.22	65.4	27.1	1126	24.9	0.138
P-6	<2 μm	84.8	171	0.792	43.9	21	402	18.1	0.044
	2–5 μm	62.1	224	1.52	63.5	29.1	607	24	0.079
	5–10 μm	82.8	939	1.85	83.2	42.5	960	29	0.150
	10–50 μm	78.6	662	1.95	77.2	44.8	904	27.6	0.158
	50–74 μm	52.3	524	1.29	50.1	24.9	463	18.6	0.104
P-7	<2 μm	68.5	149	0.534	59.3	21.8	226	21.6	0.031
	2–5 μm	37.7	120	0.167	74	38	139	28	0.056
	5–10 μm	44.3	147	0.458	88.5	46.5	158	33.5	0.054
	10–50 μm	46.7	189	0.464	92.5	49	162	34	0.071
	50–74 μm	60.3	236	1.16	87.3	43.3	346	31.5	0.170
P-8	<2 μm	25.2	69.5	0.245	67.9	23.4	69.1	22.2	0.031
	2–5 μm	37.7	117	0.263	76.7	38.1	74.7	29.4	0.093
	5–10 μm	43.5	148	0.615	81.2	45.7	90.8	31.3	0.126
	10–50 μm	43.9	184	0.344	88.7	46.8	102	32	0.170
	50–74 μm	46.7	148	0.531	85.2	47.2	91.9	29.4	0.146
P-9	<2 μm	28.2	94.1	0.43	68.7	25.5	141	24.2	0.024
	2–5 μm	37.7	150	0.627	78.2	35.6	113	30.9	0.107
	5–10 μm	44.7	195	0.525	96.2	45	140	36.3	0.137
	10–50 μm	47.3	251	0.586	99.4	48.7	151	35.2	0.190
	50–74 μm	48.5	167	0.35	76.7	52.3	171	33.4	0.121
P-10	<2 μm	59.5	102	0.369	55.4	17	117	23	0.089
	2–5 μm	47.3	195	1.26	84	33.4	301	28.8	0.122
	5–10 μm	97.5	258	1.36	106	43.7	398	32.8	0.198
	10–50 μm	56.4	302	1.14	94.1	43.4	383	31.9	0.243
	50–74 μm	47.6	180	0.578	96	46.9	134	33.2	0.213
Minimum		24.6	69.5	0.167	43.9	17	52.4	18.1	0.024
Maximum		259	5064	33.8	171	88.1	4769	41.2	0.771
Median		54.35	1	0.756	86.25	43.7	198.5	29.7	0.111

Table 2 (continued)

Sample	Particle size fractions	Contents of heavy metals/ mg kg⁻¹							
		Cu	Zn	Cd	Cr	Ni	Pb	Y	Hg
Mean		72.44	645.15	3.96	89.85	45.33	994.06	29.26	0.157
Background in Beijing		23.1	24.1	25.1	26.1	27.1	28.1		0.0576
Mean/background in Beijing		3.14	26.77	0.16	3.44	1.67	35.38		2.72
SD		51.71	1127.31	8.30	27.35	17.84	1444.14	5.49	0.16
Skewness		2.36	3.08	2.89	1.14	0.80	1.67	−0.16	2.43
Kurtosis		5.74	9.17	7.38	1.54	0.28	1.41	−0.32	6.53

are presented in a dendrogram (Fig. 4), representing the hierarchical clustering solution and values of the distances between clusters (squared Euclidean distance). Correlation coefficients were used to identify the relationship between the 10 elements. Pearson's product moment correlation coefficient was calculated in the forms of matrices (Kotz et al. 1984). Other statistical parameters, such as the range, mean, median, standard deviation, standard error, skewness, kurtosis, and coefficient of variation, were computed using SPSS 16.0.

The particle size fractions result in a tri-dimensional structure with an X, a parallelepiped of size ($n_{frac} \times n_{met} \times n_{samp}$), n_{samp} being the number of objects (sampling sites), n_{met} the number of variables (trace elements and heavy metals), and n_{frac} the number of particle size fractions. The X can be unfolded to be X^{aug} with dimensions that can then be subjected to 2-PCA. This method, which is known as MA-PCA, is commonly used to analyze environmental science data (Guevara-Riba et al. 2004; Jain 2004). Although MA-PCA allows full recovery of the

Fig. 2 Mean contents (mg kg⁻¹) of selected essential trace elements in five particle size fractions (μm) (n=10)
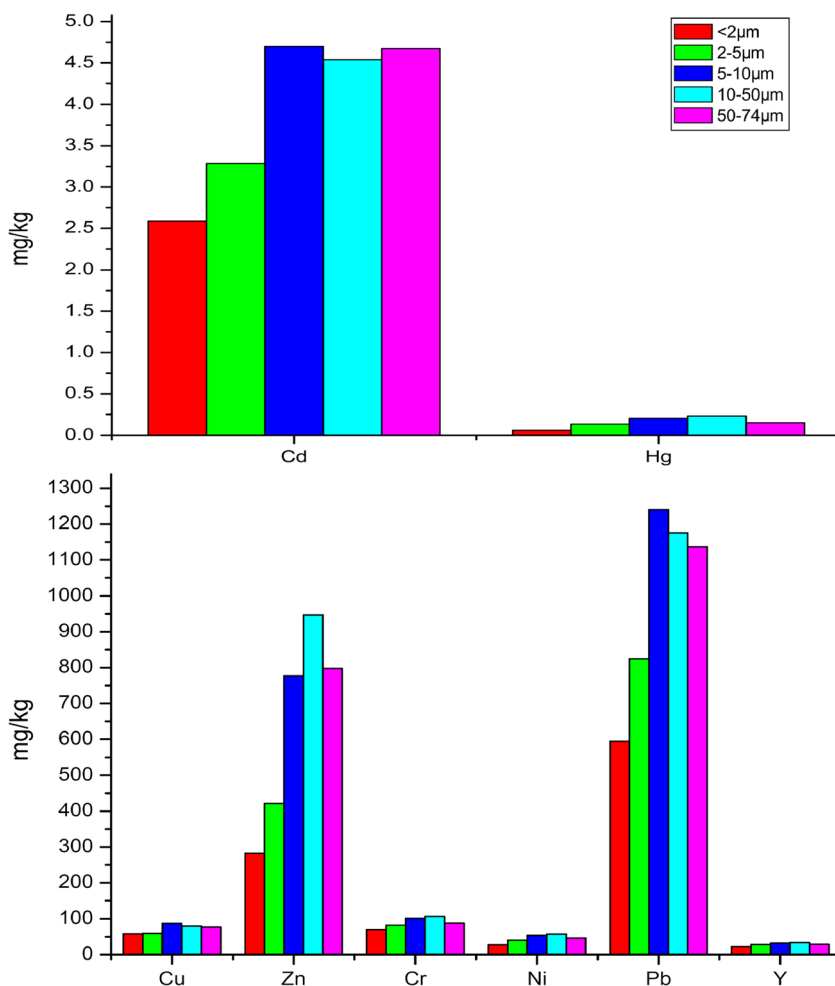
Table 3 Correlation coefficients for trace elements, organic matter, and pH in the surface soils of the study area

	Cu	Zn	Cd	Cr	Ni	Pb	As	Hg	pH	OM
Cu	1.000									
Zn	0.586[a]	1.000								
Cd	0.623[a]	0.994[a]	1.000							
Cr	−0.062	−0.094	−0.108	1.000						
Ni	0.135	0.155	0.144	0.948[a]	1.000					
Pb	0.282	0.748[a]	0.694[a]	−0.047	0.086	1.000				
As	0.429[b]	0.865[a]	0.832[a]	−0.074	0.099	0.970[a]	1.000			
Hg	0.217	0.527[a]	0.501[b]	−0.151	−0.053	0.530[a]	0.544[a]	1.000		
pH	−0.087	−0.028	−0.022	−0.148	−0.207	−0.018	−0.013	0.018	1.000	
OM	0.345	0.729[a]	0.736[a]	−0.046	0.187	0.236	0.366	0.490[b]	−0.129	1.000

[a] Correlation is significant at the 0.01 level (2-tailed)

[b] Correlation is significant at the 0.05 level (2-tailed)

information from the variables, the information from samples and fractions becomes mixed (Pardo et al. 2004). Conversely, N-way PCA, which is an extension of 2-PCA to higher orders, accounts for the true tri-dimensional nature of X. As a result, the information corresponding to each of the three dimensions or ways, metals, samples, and fractions can be fully separated and interpreted. The Tucker 3 model is the most commonly used N-way model and has frequently been utilized to evaluate environmental data (Pardo et al. 2004; Singh et al. 2006). This method decomposes X according to (Henrion 1994):

$$X_{ijk} = \sum_{p=1}^{P} \sum_{q=1}^{Q} \sum_{r=1}^{R} a_{ip}b_{jq}c_{kr}g_{pqr} + e_{ijk}$$

where a_{ip}, b_{jq}, and c_{kr} are the elements of the loading matrixes A, B, and C with ($n_{frac} \times P$), ($n_{met} \times Q$), and ($n_{samp} \times R$) dimensions, respectively. g_{pqr} denotes the elements (p, q, r) of the core array G ($P \times Q \times R$), and e_{ijk} is the error term of the element x_{ijk} in the X dataset.

Correlation analysis

Inter-element relationships of total heavy metal contents not only provide interesting information regarding the sources and pathways of the heavy metals, but can also be applied to explain the behavior and fate of heavy metals effectively and efficiently (Yalcin et al. 2008; Yalcin et al. 2010).

The results of the correlations between heavy metals, pH, and OM illustrate different origins and behaviors of trace elements in bulk samples (Table 3). The coefficients calculated for bulk samples indicated there is no correlation between any of the metals and the pH, indicating that pH almost no impact on distribution of heavy metals. The reason may be that the waste rock and tailings in the study area accumulation has been for decades, and some of the metal is easily influenced by the pH has been moved due to the leaching effect or other effects. The rest of the metals have more stable structure. The significant positive correlation between As, Zn, Cd, and Pb is

Table 4 Principal component loadings of selected metals in the bulk and size fractions soil sample soils

| Bulk sample				Size fractions soil samples			
	1	2			1	2	3
Total	4.254	1.969		Total	4.833	1.787	1.019
% of Variance	53.179	24.611		% of Variance	60.407	22.342	12.739
Cumulative %	53.179	77.790		Cumulative %	60.407	82.749	95.488
Cu	0.603	0.064		Cu	0.895	−0.341	0.136
Zn	0.959	0.027		Zn	0.928	−0.309	0.085
Cd	0.942	0.018		Cd	0.894	−0.371	−0.020
Cr	−0.098	0.982		Cr	0.594	0.740	−0.262
Ni	0.125	0.986		Ni	0.775	0.598	−0.114
Pb	0.865	0.000		Pb	0.851	0.121	−0.471
As	0.946	−0.001		Y	0.144	0.685	0.704
Hg	0.643	−0.168		Hg	0.819	−0.222	0.440

consistent with a common source for these metals. Cr and Ni showed a significant positive correlation.

Principal component analysis

We used PCA to identify the sources of pollutants. To reveal the origins of trace elements and their intrinsic relations, we analyzed the concentrations of Cu, Zn, Cd, Cr, Ni, Pb, As, and Hg from 25 bulk soils and the concentrations of Cu, Zn, Cd, Cr, Ni, Pb, Y, and Hg from 50 size fractions samples.

Table 4 shows the results of factor loadings with a varimax rotation, as well as the eigenvalues and communalities in the bulk and size fractions of soil samples. The results indicate that there were two eigenvalues higher than 1, and these two factors explain 77.79 % of the total variance in bulk soil samples. The first factor explains 53.18 % of the total variance and loads heavily on Zn, Cd, As, and Pb. The second principal component (PC2) revealed higher contributions of Cr and Ni, accounting for 24.61 % of the total variance. The relationships among heavy metals based on the first two principal components are illustrated in Fig. 3a.

Fig. 3 PCA results in the two or three-dimensional space: plot of loading of the first two principal components (**a** bulk soils); plot of loading of the first three principal components (**b** size fractions soils)
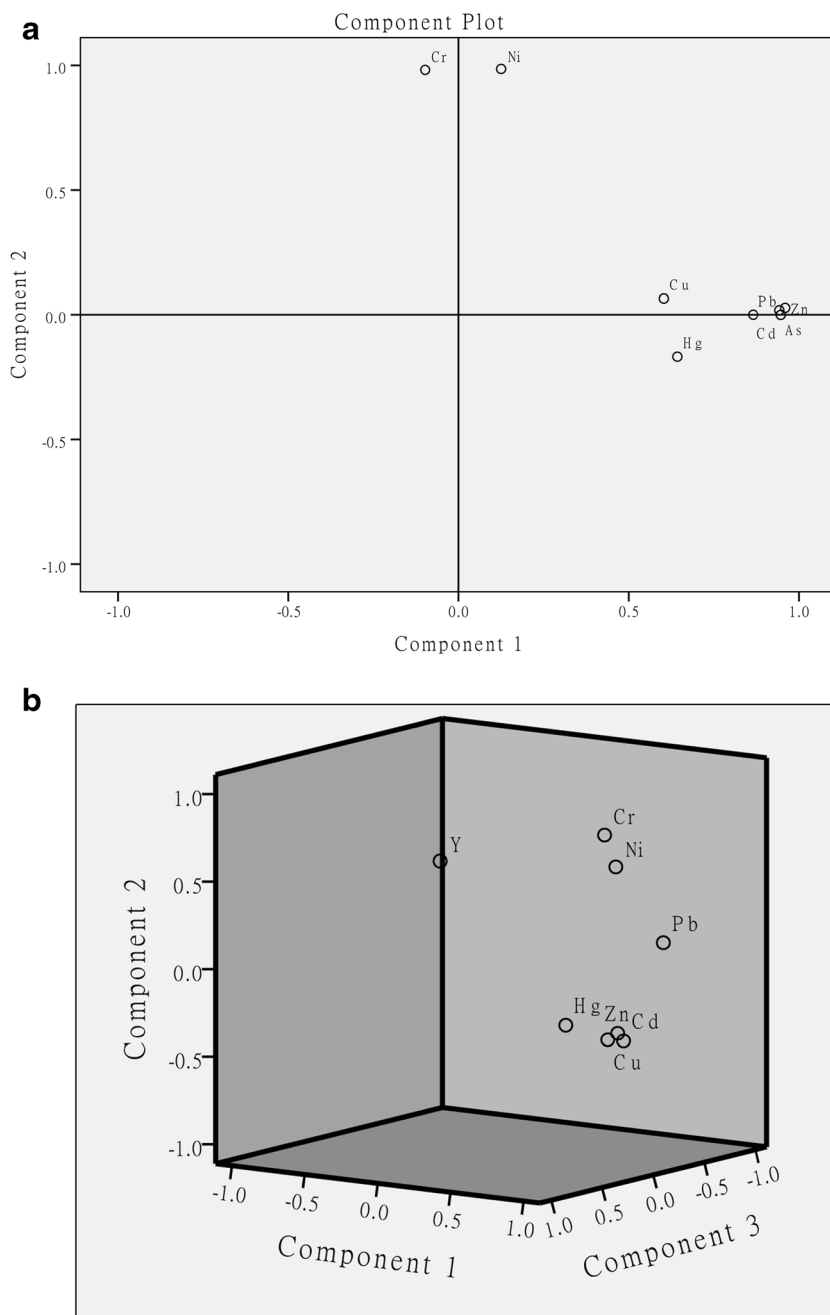
Three PCs with eigenvalues greater than 1 were obtained for the size fractions, together explaining more than 95.49 % of the variance. The first PC exhibited elevated loadings of Cu, Zn, Cd, Ni, Pb, and Hg, while PC 2 indicated significant loadings in favor of Cr, Ni, and Y and PC 3 revealed higher contributions of Y. The relationships among heavy metals based on the first three principal components are illustrated in Fig. 3b in three-dimensional space.

Cluster analysis

The heavy metal concentration data were standardized by means of z-scores before CA, and Euclidean distances for similarities in the variables were calculated. Hierarchical clustering was then conducted by applying Ward's method to the standardized data set (Sundaray et al. 2006).

The CA results of bulk soils revealed three clusters of elements (Fig. 4). The first cluster (C1) included elements that had previously been interpreted as anthropogenic elements (Zn, Cd, Pb, and As), while the second cluster (C2) contained Cu and Hg and the third cluster (C3) consisted of Cr and Ni, while Cr and Ni had been interpreted as a mixed source element.

Tucker analysis

The scaled data were analyzed using the Tucker 3 model (Bro and Smilde, 2003). The first step in Tucker analysis is selection of an optimal model in terms of complexity. This is done to identify a model that explains the highest percentage of variance using the least latent factors in each mode. To select the optimal model, we calculated the percentage of the explained variance for all models according to the product, starting from one factor in each mode, [1 1 1] to [5 8 10]. As shown in Fig. 5, [2 3 3] explained 87.1 % of the total data variance. A further increase in terms better explained the variance, but made the models too difficult to interpret. Therefore, [2 3 3] was selected as the optimal model for this paper.

To fully separate the information provided in the Tucker 3 model, the structure of the core matrix, G (Leardi et al. 2000), must be also considered. In our case, model [2 3 3] generated the following core matrix:

| g111	g121	g131	g211	g221	g231
−14.2823	1.8796	1.249	−0.158	−0.2436	−1.7378
g112	g122	g132	g212	g222	g232
0.6484	3.6791	−3.5845	−4.2488	−4.223	−2.9474
g113	g123	g133	g213	g223	g233
−0.3156	−6.2033	1.0942	−2.7067	−1.6702	−2.8487

Figure 6 shows a summary of the components of the Tucker 3 [2 3 3] model, which was composed of the loadings of the three matrixes, particle fractions (A), metals (B), and samples (C). There were two factors in model A and three factors for both the metals and samples (models B and C, respectively).

In model A (particle fraction), the first factor (A1) was composed of highly positive loadings for 5–10, 10–50, and 50–74 μm with larger magnitudes, but also with smaller magnitudes (<2 and 2–5 μm). We believe that heavy metals are mainly distributed in the larger particle size of soil and lower in the smaller particle sizes, which is consistent with the metal content distribution shown in Fig. 2. Heavy metals in large particle size soil are usually from mineral constituents. It can be assumed that the heavy metals observed in the present study originated from gold mining. Fine particulate matter can migrate with the atmosphere, so the heavy metals in the fine particles of the soil can be easily influenced by atmospheric deposition. This resulted the difference between the heavy metals in the fine particles and in the other particles.

The first component (B1) of the B model had negative loadings for all metals, with Y having the lowest value. Y is generally attributed to compounds originating from the earth's crust, while being less affected by anthropogenic actives; therefore, it may be considered representative of the natural sources. In the first main component, there is a great difference between loadings of Y and other elements. It is believed that other elements are largely influenced by anthropogenic factors, which result in the differences. In the second component (B2), Cr, Ni, Pb, and Y have negative loadings. It can be assumed that Cr, Ni, and Pb were partially affected by natural sources, while Cu, Zn, Cd, and Hg were less influenced by these. In the third component (B3), Y and Hg show greater negative loadings, indicating that Hg and Y also showed consistent characteristics in a few test results, which may have been derived from natural sources.

The first component (C1) of the C model had negative loadings for all metals except P-1, P-2, and P-5. All metal content was high in P-1 and P-2; however, P-5 showed a similar metal distribution as P-1 and P-2. While P-1 and P5 are both in area surrounding the gold mines, P-5 was located farther away. However, the elevation of P-1, P-2, and P-5 was higher than that of P-3 and P-4. Moreover, P-3 and P-4 were located close to the road and subject to frequent traffic activities, resulting in the difference between these samples and the others. Loading in the second component (C2), P-1, which was located nearest to the mining activities, was the only one that showed negative loading. This

Fig. 4 Cluster analysis of selected metals in the bulk soil samples
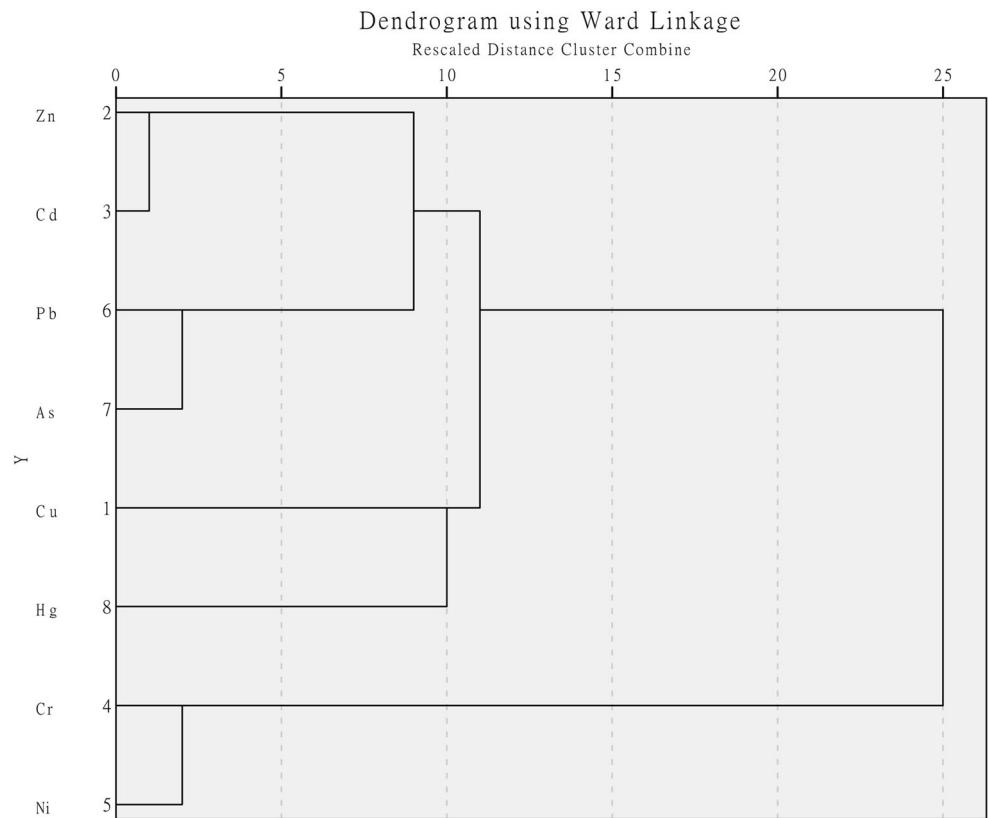
Fig. 5 Explained percentage of variance versus model dimensionality as determined by Tucker 3 modeling of the particle size fractions result
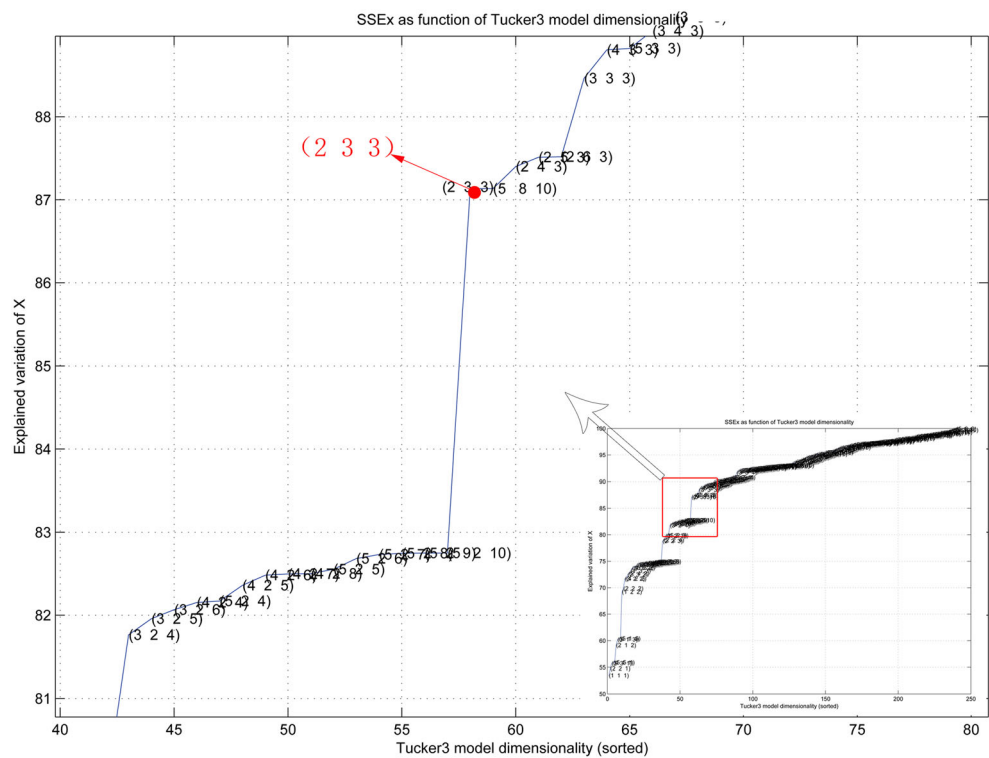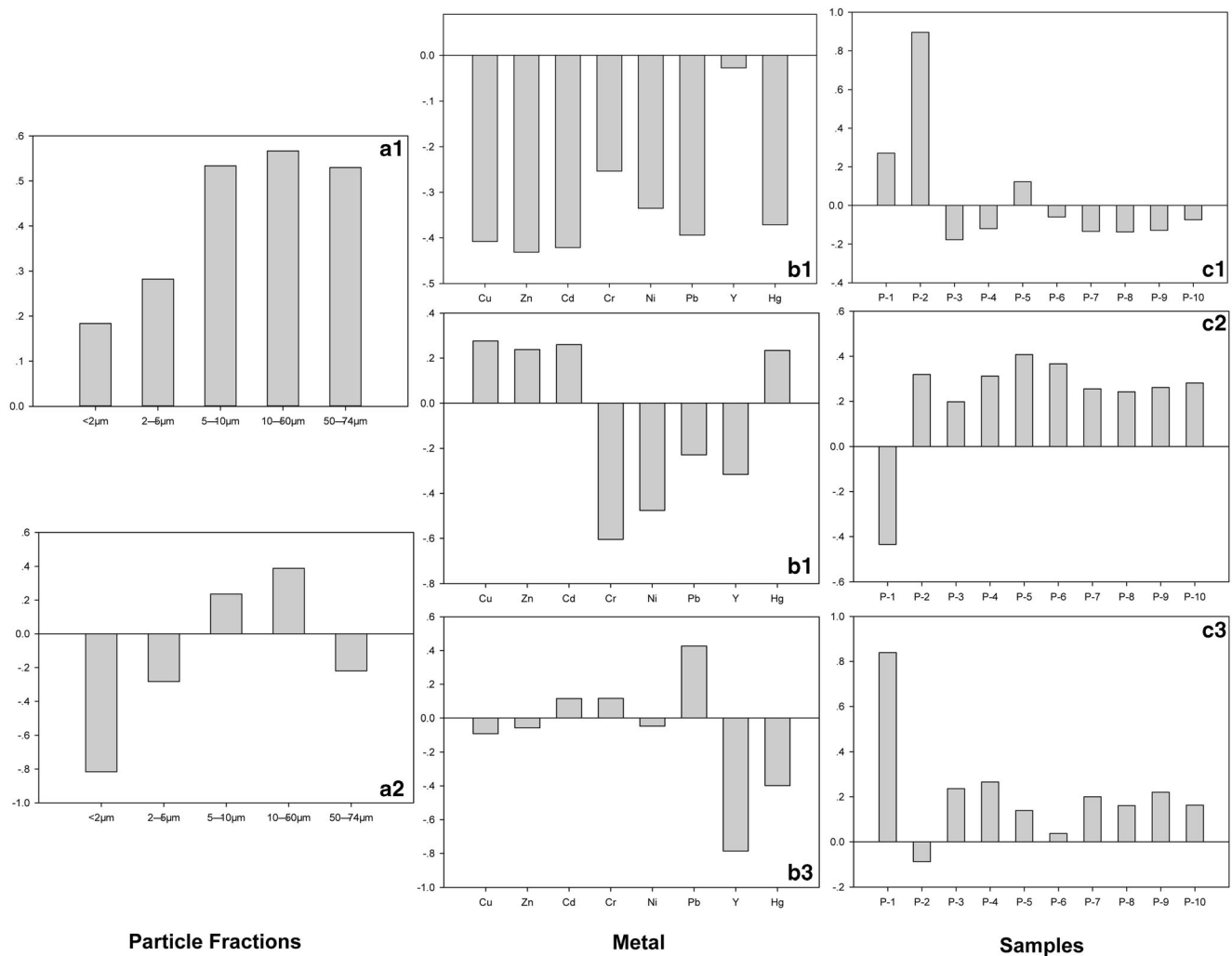
Fig. 6 Loadings of the Tucker 3 [2 3 3] model of the particle size fractions result

indicates that the heavy metal content of P-1 was significantly different from that of other sampling points. However, in the third component (C3), P-2 and P-1 showed opposite loadings, indicating that P-2 is not only affected by mining, but also by other factors.

Discussion

Pollution degree and source identification

High levels of As may be caused by the mining residue. Elevated As concentrations in the residues are associated with the inherent mineralogy of the ores which contain arsenopyrite (FeAsS) (De Lacerda and Salomons 2012), a mineral normally associated with significant amounts of gold, serving as an indicator of gold bearing reefs. Runoff and wind could transport particles rich in As to the surroundings.

The result of total Cd, Pb, and As in the study area suggests that these metals were higher than the background in Beijing (Zhongming et al. 1990). Cu, Zn, Cr, and Ni are similar to those previously exposed by Huang et al. (2013) and Qin et al. (2014). While Pb and As are higher than those previously exposed by Huang et al. (2013) and Qin et al. (2014), especially As, nearly 10 times the value of previous reports in the adjacent area (Qin et al. 2014; Huang et al. 2013). Values of As reported in this study are similar to those previously exposed by Faz et al.(2014) in primary gold mining districts of Western Bolivia.

In fact, Tapia et al. (2012) also observed in the Oruro mining district of Bolivia that backgrounds of As are significantly enhanced in comparison with the upper continental crust concentrations and those of industrial sites, suggesting that surface soils are probably influenced by mining activities and impacted by airborne particulates.
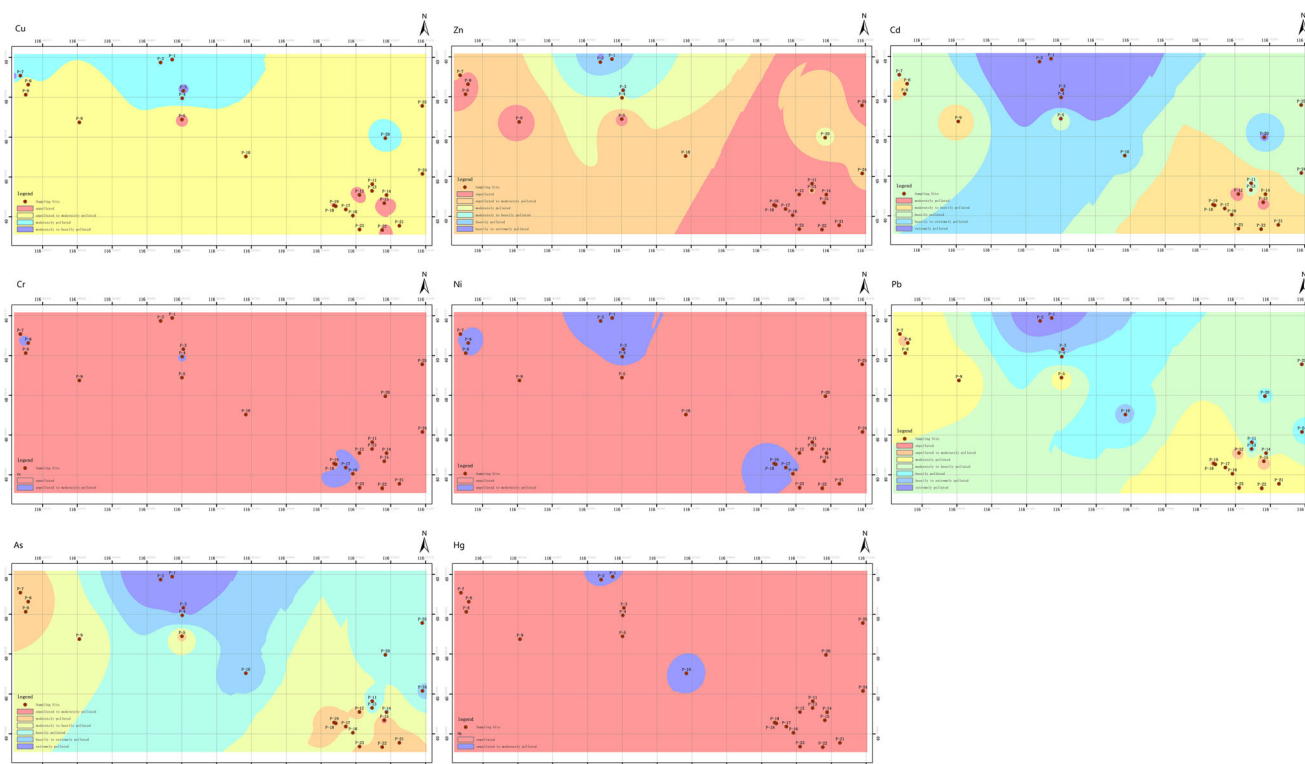
Fig. 7 Distribution maps of concentrations of trace elements in the topsoil

The results of chemometric analysis show that As, Zn, Cd, and Pb have similar content characteristics (correlation analysis, PCA, and CA all show this result). These metals may be affected by the mine, resulting in higher levels. We refer to the ore composition test report, the content of As reached 0.36 %, and this is consistent with our conjecture. It has been reported that the availability and mobility of As is highly dependent on the parent mineral form (Al-Abed et al. 2008).

Generally, the parent rock has larger particle size in soil, while in smaller grain size soil easily influenced by wind erosion and other factors, it is often a source of a variety of effects. Figure 2 shows that Zn, Cd, and Pb in the larger grain size were significantly higher than in fine particle size. We can deduce that Zn, Cd, and Pb may mainly from the parent rock influenced by mining activities in this study. This inference is consistent with the results of previous chemometric analysis.

In order to further analyze the potential relationship between particle size, sampling point, and metal content, the Tucker 3 model is used to process the tri-dimensional dataset. The results also show that it has a greater correlation between the larger grain sizes of the soil particles. In addition, Pb affected by mining activities, also seems to be affected by other factors, showed slight differences with Pb and Zn. From the results of the sample point analysis, it can be seen that P-3, P-4 points near the road with lower altitude show

different characteristics with other high concentration points, and we hypothesized that road is an important factors influencing the metal distribution in p-3, p-4 points. In the previous reports (Birch and Scollen 2003; Ning et al. 2010; Liu et al. 2014), the Pb elements in the soil around the road were significantly enriched and usually enriched at a distance of less than 500 m from the road.

Risk assessment

The geo-accumulation index is a quantitative measure of the pollution index in soils. The contamination level was assessed by comparing the observed heavy metal levels in soils to the background concentrations of metals in Beijing soils. Any increase in observed levels indicates an anthropogenic nature of the observed metal. The natural fluctuations in the metal contents of the soils are countered by a constant factor 1.5.

Table 5 Reference values (C_n^i) and toxicity coefficient (T_r^i) of heavy metals in soils

	Cu	Zn	Cd	Cr	Ni	Pb	As	Hg
C_n^i	23.1	97.2	0.0534	66.7	28.2	24.7	9.4	0.0576
T_r^i	5	1	30	2	5	5	10	40

Table 6 Grading standard of the potential ecological risk for heavy metals (Hakanson 1980)

| E_r^i	Potential ecological risk for single regulator	RI	Ecological risk for all factors
$E_n^i < 40$	Low	RI < 150	Low
$E_n^i \geq 40$	Moderate	RI ≥ 150	Moderate
$E_n^i \geq 160$	Considerable	RI ≥ 300	High
$E_n^i \geq 320$	High	RI ≥ 600	Very high

We also mapped the distributions of Igeo in soils. Thus, the impact of the soils was assessed by developing an individual pollution map for each element found in bulk samples. The distribution patterns of Cu, Zn, Cd, Cr, Ni, Pb, Hg, and As were prepared using ARCGIS 10.2 by the interpolation method with inverse distance weighting (Zhu et al., 2013). The pollution spatial distribution patterns of trace elements in soils are shown in Fig. 7.

As shown in Fig. 7, Zn, Pb, and As showed a uniform distribution, differing from the pollution-derived elements. Overall, these results indicate serious pollution with metals in the mine area.

The potential ecological risk index of Hakanson was evaluated by eight parameters (Hg, Cd, As, Pb, Cu, Cr, Zn, and PCBs). However, PCBs were excluded, and the Ni was added in this study. The soil background values in Beijing (China National Environmental Monitoring Centre, 1990) were adopted as reference values. The reference values and the toxic response factors are shown in Table 5. The evaluated criteria for the individual potential ecological factor E_r^i and potential ecological index (RI) are shown in Table 6. The potential ecological indices E_r^i and RI in surface sediments are shown in Table 7. The results indicated moderate to very high potential risk for all sites, where the RI

Table 7 Heavy metals ecological risk indexes of the study area

Samples	E_r^i								RI
	Cu	Zn	Cd	Cr	Ni	Pb	As	Hg	
P-1	17.25	17.28	7865.17	2.80	7.82	1291.50	2538.30	67.36	11,807.48
P-2	26.19	25.31	13,033.71	2.36	8.01	474.70	1360.64	81.25	15,012.17
P-3	37.88	13.07	7977.53	2.55	7.50	188.66	937.23	26.39	9190.81
P-4	15.54	4.86	2556.18	3.12	8.19	67.81	389.36	16.67	3061.73
P-5	6.49	1.21	449.44	2.70	6.37	18.54	50.00	15.28	550.04
P-6	13.16	1.41	342.70	3.18	8.92	13.68	38.30	26.39	447.73
P-7	35.28	1.77	601.12	2.49	6.35	19.72	53.19	26.39	746.31
P-8	10.04	1.21	280.90	2.80	6.84	15.79	36.17	32.64	386.40
P-9	7.79	1.21	258.43	2.58	5.80	17.77	60.64	52.08	406.31
P-10	13.14	1.87	820.22	2.49	5.50	132.59	336.17	91.67	1403.65
P-11	10.63	1.13	376.40	2.21	4.31	73.08	174.47	39.58	681.81
P-12	5.74	0.74	106.74	2.87	6.44	8.72	42.55	7.64	181.44
P-13	10.04	1.74	646.07	2.34	5.07	86.23	204.26	26.39	982.14
P-14	8.03	0.91	314.61	2.01	4.22	52.23	138.30	55.56	575.86
P-15	5.97	0.76	123.60	2.61	6.22	6.94	23.40	8.33	177.84
P-16	7.62	1.15	275.28	2.87	6.97	27.53	93.62	13.89	428.92
P-17	12.75	1.21	224.72	5.31	16.19	19.47	56.38	29.86	365.90
P-18	8.40	1.11	252.81	2.93	8.00	19.35	59.57	27.78	379.95
P-19	6.99	0.93	196.63	2.77	7.77	12.67	41.49	21.53	290.77
P-20	22.94	3.76	1550.56	2.31	5.59	64.98	226.60	20.14	1896.87
P-21	8.61	1.06	202.25	2.74	6.86	15.85	30.85	16.67	284.89
P-22	6.71	1.01	230.34	2.69	5.92	20.45	52.13	27.08	346.33
P-23	10.13	1.32	258.43	2.27	6.06	19.29	56.38	16.67	370.55
P-24	12.21	1.97	573.03	2.57	6.10	85.63	288.30	37.50	1007.30
P-25	7.62	1.34	601.12	2.06	4.08	48.79	181.91	22.22	869.14
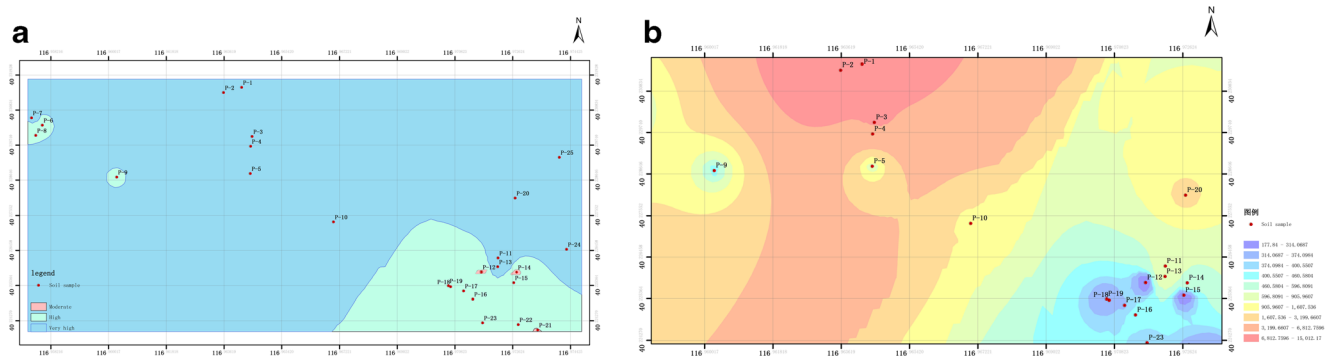
Fig. 8 Spatial distribution map of RI in the study area: the distribution of moderate ecological risk to very high risk (**a**); natural grade distribution potential ecological risks (**b**, 10 grades)

values are all higher than 150. P-12, P-15, P-19, and P-21 showed moderate ecological risk, while P-5–6, P-8–9, P-14, P-16–18, and P22–23 showed high ecological risk. The rest of the sites showed very high ecological risk. The order of potential ecological risk factor E_r^i of heavy metals in soils was Cd>As>Pb>Hg>Cu>Ni>Zn>Cr. As, Pb, and Cd showed the highest potential ecological risk factor, while the rest had lower potential ecological risk factors. Therefore, As, Pb, and Cd should receive a great deal of attention as ecological hazards and be considered priority pollutants. The count map of RI for the studied area based on the contents of Hg, Cd, As, Pb, Cu, Cr, Zn, and Ni is shown in Fig. 8. As shown in Fig. 8a, most of the study area had very high potential ecological risk, a small part had high potential ecological risk, and only a few sampling points on the perimeter had moderate ecological risk. As shown in Fig. 8b, the potential ecological risk increased closer to the mining area.

Conclusions

Mining activities in the upstream areas of the Zhongqiao Reservoir have caused serious heavy metals contamination of soils. This was especially true for Cd, As, and Pb, for which observed values were much higher than the background values. The lowest metal content was observed in the <2 μm size fraction, while the concentration of each trace element increased in larger particles, then decreased in the 50–74 μm size fraction. According to multivariate analysis (correlation coefficient analysis, PCA, CA) and the contents of selected metals, Zn, Cd, As, and Pb originated from anthropogenic sources in bulk soil, while Cr and Ni had natural and anthropogenic origins. The geo-accumulation index demonstrated moderate to high contamination of a few metal bulk soil samples. Overall, these findings indicate that gold mining activities have the potential to adversely affect drinking water

sources of Beijing and should therefore receive increased attention.

References

Acosta J, Faz A, Mart Nez-Mart Nez S, Zornoza R, Carmona D, Kabas S (2011) Multivariate statistical and GIS-based approach to evaluate heavy metals behavior in mine sites for future reclamation. J Geochem Explor 109:8–17

Ahmed F, Ishiga H (2006) Trace metal concentrations in street dusts of Dhaka city, Bangladesh. Atmos Environ 40:3835–3844

Al-Abed SR, Jegadeesan G, Scheckel KG, Tolaymat T (2008) Speciation, characterization, and mobility of As, Se, and Hg in flue gas desulphurization residues. Environ Sci Technol 42:1693–1698

Baek S-O, Choi J-S, Hwang S-M (1997) A quantitative estimation of source contributions to the concentrations of atmospheric suspended particulate matter in urban, suburban, and industrial areas of Korea. Environ Int 23:205–213

Barberis E, Marsan FA, Boero V, Arduino E (1991) Aggregation of soil particles by iron oxides in various size fractions of soil B horizons. J Soil Sci 42:535–542

Birch G, Scollen A (2003) Heavy metals in road dust, gully pots and parkland soils in a highly urbanised sub-catchment of Port Jackson, Australia. Soil Res 41:1329–1342

Brady NC, Weil RR (1996) The nature and properties of soils. Prentice-Hall Inc, Upper Saddle River

Bro R, Smilde AK (2003) Centering and scaling in component analysis[J]. J Chemom 17(1):16–33

Charlesworth S, Lees J (1999) Particulate-associated heavy metals in the urban environment: their transport from source to deposit, Coventry, UK. Chemosphere 39:833–848

De Lacerda LD, Salomons W (2012) Mercury from gold and silver mining: a chemical time bomb? Springer Science & Business Media. doi:10.1007/978-3-642-58793-1

Ding H, Ji H (2010) Application of chemometric methods to analyze the distribution and chemical fraction patterns of metals in sediment from a metropolitan river. Environ Earth Sci 61:641–657

Dominici F, Peng RD, Bell ML, Pham L, Mcdermott A, Zeger SL, Samet JM (2006) Fine particulate air pollution and hospital admission for cardiovascular and respiratory diseases. JAMA 295:1127–1134

Facchinelli A, Sacchi E, Mallen L (2001) Multivariate statistical and GIS-based approach to identify heavy metal sources in soils. Environ Pollut 114:313–324

Farnham I, Johannesson K, Singh A, Hodge V, Stetzenbach K (2003) Factor analytical approaches for evaluating groundwater trace element chemistry data. Anal Chim Acta 490:123–138

Faz Á, Zornoza R, Muñoz MÁ, Acosta JA (2014) Metals and metalloids in primary gold mining districts of Western Bolivia: anthropogenic and natural sources. Environ Earth Sci 71:5027–5036

Förstner U, Wittmann GTW (2012) Metal pollution in the aquatic environment. Springer Science & Business Media. doi:10.1007/978-3-642-69385-4

Gao Y-X, Feng J-G, Tang L, Zhu X-F, Liu W-Q, Ji H-B (2012) Fraction distribution and risk assessment of heavy metals in iron and gold mine soil of Miyun Reservoir upstream. Environ Sci 33:1707–1717

Guevara-Riba A, Sahuquillo A, Rubio R, Rauret G (2004) Assessment of metal mobility in dredged harbour sediments from Barcelona, Spain. Sci Total Environ 321:241–255

Guo W, Zhao R, Zhang J, Bao Y, Wang H, Yang M, Sun X, Jin F (2011) Distribution characteristic and assessment of soil heavy metal pollution in the iron mining of Baotou in Inner Mongolia. Environ Sci (in Chinese) 32:3099–3105

Hakanson L (1980) An ecological risk index for aquatic pollution control. A sedimentological approach. Water Res 14:975–1001

Henrion R (1994) N-way principal component analysis theory, algorithms and applications. Chemom Intell Lab Syst 25:1–23

Huang X, Zhu Y, Ji H (2013) Distribution, speciation, and risk assessment of selected metals in the gold and iron mine soils of the catchment area of Miyun Reservoir, Beijing, China. Environ Monit Assess 185:8525–8545

Jain C (2004) Metal fractionation study on bed sediments of River Yamuna, India. Water Res 38:569–578

Kaiser HF (1960) The application of electronic computers to factor analysis. Educ Psychol Meas 20:141–151. doi:10.1177/001316446002000116

Kotz S, Pearn W, Wichern DW (1984) Eigenvalue-eigenvector analysis for a class of patterned correlation matrices with an application. Stat Probab Lett 2:119–125

Leardi R, Armanino C, Lanteri S, Alberotanza L (2000) Three-mode principal component analysis of monitoring data from Venice lagoon. J Chemometr 14:187–195

Li Y (2004) Simultaneous determination of Arsenic and Mercy in soil by atomic fluorescence spectrometry with hydride generation. Agro-Environment and Development 1:41–42

Li Z, Ma Z, van der Kuijp TJ, Yuan Z, Huang L (2014) A review of soil heavy metal pollution from mines in China: pollution and health risk assessment. Sci Total Environ 468:843–853

Lin Y-P, Teng T-P, Chang T-K (2002) Multivariate analysis of soil heavy metal pollution and landscape pattern in Changhua county in Taiwan. Landsc Urban Plan 62:19–35

Liu C-P, Luo C-L, Gao Y, Li F-B, Lin L-W, Wu C-A, Li X-D (2010) Arsenic contamination and potential health risk implications at an abandoned tungsten mine, southern China. Environ Pollut 158:820–826

Liu E, Yan T, Birch G, Zhu Y (2014) Pollution and health risk of potentially toxic metals in urban road dust in Nanjing, a mega-city of China. Sci Total Environ 476:522–531

Meza-Figueroa D, de La O-Villanueva M, de la Parra ML (2007) Heavy metal distribution in dust from elementary schools in Hermosillo, Sonora, México. Atmos Environ 41:276–288

Muller G (1969) Index of geoaccumulation in sediments of the Rhine River. Geol J 2(3):108–118

Ning Z, Hudda N, Daher N, Kam W, Herner J, Kozawa K, Mara S, Sioutas C (2010) Impact of roadside noise barriers on particle size distributions and pollutants concentrations near freeways. Atmos Environ 44:3118–3127

Pardo R, Helena B, Cazurro C, Guerra C, Deban L, Guerra C, Vega M (2004) Application of two-and three-way principal component analysis to the interpretation of chemical fractionation results obtained by the use of the BCR procedure. Anal Chim Acta 523:125–132

Pardo R, Vega M, Deb NL, Cazurro C, Carretero C (2008) Modelling of chemical fractionation patterns of metals in soils by two-way and three-way principal component analysis. Anal Chim Acta 606:26–36

Perona E, Bonilla I, Mateo P (1999) Spatial and temporal changes in water quality in a Spanish river. Sci Total Environ 241:75–90

Qin F, Ji H, Li Q, Guo X, Tang L, Feng J (2014) Evaluation of trace elements and identification of pollution sources in particle size fractions of soil from iron ore areas along the Chao River. J Geochem Explor 138:33–49

Qishlaqi A, Moore F (2007) Statistical analysis of accumulation and sources of heavy metals occurrence in agricultural soils of Khoshk River Banks, Shiraz, Iran. Am Eurasian J Agric Environ Sci 2:565–573

Salman S, Ruka'h YA (1999) Multivariate and principal component statistical analysis of contamination in urban and agricultural soils from north Jordan. Environ Geol 38:265–270

Singh KP, Malik A, Singh VK, Sinha S (2006) Multi-way data analysis of soils irrigated with wastewater–A case study. Chemom Intell Lab Syst 83:1–12

Stanimirova I, Zehl K, Massart D, Vander Heyden Y, Einax J (2006) Chemometric analysis of soil pollution data using the Tucker N-way method. Anal Bioanal Chem 385:771–779

Sterckeman T, Douay F, Proix N, Fourrier H (2000) Vertical distribution of Cd, Pb and Zn in soils near smelters in the North of France. Environ Pollut 107:377–389

Sundaray SK, Panda UC, Nayak BB, Bhatta D (2006) Multivariate statistical techniques for the evaluation of spatial and temporal variations in water quality of the Mahanadi river–estuarine system (India)–a case study. Environ Geochem Health 28:317–330

Tahri M, Benyaich F, Bounakhla M, Bilal E, Gruffat J-J, Moutte J, Garcia D (2005) Multivariate analysis of heavy metal contents in soils, sediments and water in the region of Meknes (central Morocco). Environ Monit Assess 102:405–417

Tapia J, Audry S, Townley B, Duprey J-L (2012) Geochemical background, baseline and origin of contaminants from sediments in the mining-impacted Altiplano and Eastern Cordillera of Oruro, Bolivia. Geochem: Explor, Environ, Anal 12:3–20

Vallejo M, Ruiz S, Hermosillo AG, Borja-Aburto VH, Cárdenas M (2006) Ambient fine particles modify heart rate variability in young healthy adults. J Expo Sci Environ Epidemiol 16:125–130

Viklander M (1998) Particle size distribution and metal content in street sediments. J Environ Eng 124:761–766

Webster R, Oliver MA (1990) Statistical methods in soil and land resource survey. Oxford University Press (OUP). doi:10.2307/2290549

Xu ZQ, Ni SJ, Tuo X, Zhang CJ (2008) Calculation of heavy metals' toxicity coefficient in the evaluation of potential ecological risk index. Environ Sci Technol 31:112–115

Xv Y, Zhang J, Zhao A, Ke H (2008) Evaluation of the potential ecological risk of heavy metals in farmland soils in a certain gold mining area, Xiaoqinling, China. Geol Bull Chin 27:272–278

Yalcin MG, Narin I, Soylak M (2008) Multivariate analysis of heavy metal contents of sediments from Gumusler creek, Nigde, Turkey. Environ Geol 54:1155–1163

Yalcin MG, Tumuklu A, Sonmez M, Erdag DS (2010) Application of multivariate statistical approach to identify heavy metal sources in bottom soil of the Seyhan River (Adana), Turkey. Environ Monit Assess 164:311–322

Zheng Y-M, Chen T-B, He J-Z (2008) Multivariate geostatistical analysis of heavy metals in topsoils from Beijing, China. J Soils Sediments 8: 51–58

Zhongming Z, Linong L, Xiaona Y, Wangqiang Z and Wei L (1990) China National Environmental Monitoring Centre. Soil Element Background Values of China[J] (in Chinese). China Environmental Science Press

Zhu X, Ji H, Chen Y et al (2013) Assessment and sources of heavy metals in surface sediments of Miyun Reservoir, Beijing[J]. Environ Monit Assess 185(7):6049–6062

Zhuang P, Zou B, Li N, Li Z (2009) Heavy metal contamination in soils and food crops around Dabaoshan mine in Guangdong, China: implication for human health. Environ Geochem Health 31:707–715